Fixed-bed adsorption of reactive azo dye onto granular activated carbon prepared from waste

A.A. Ahmad, B.H. Hameed *

School of Chemical Engineering, Engineering Campus, Universiti Sains Malaysia, 14300 Nibong Tebal, Penang, Malaysia

A B S T R A C T

In this work, the adsorption potential of bamboo waste based granular activated carbon (BGAC) to remove C.I. Reactive Black (RB5) from aqueous solution was investigated using fixed-bed adsorption column. The effects of inlet RB5 concentration (50–200 mg/L), feed flow rate (10–30 mL/min) and activated carbon bed height (40–80 mm) on the breakthrough characteristics of the adsorption system were determined. The highest bed capacity of 39.02 mg/g was obtained using 100 mg/L inlet dye concentration, 80 mm bed height and 10 mL/min flow rate. The adsorption data were fitted to three well-established fixed-bed adsorption models namely, Adam's–Bohart, Thomas and Yoon–Nelson models. The results fitted well to the Thomas and Yoon–Nelson models with coefficients of correlation $R^2 \geq 0.93$ at different conditions. The BGAC was shown to be suitable adsorbent for adsorption of RB5 using fixed-bed adsorption column.

© 2009 Elsevier B.V. All rights reserved.

1. Introduction

Azo dyes are synthetic organic compounds widely used in textile dyeing, paper printing and other industrial processes such as the manufacture of pharmaceutical drugs, toys and foods [1]. This chemical class of dyes, which is characterized by the presence of at least one azo bond (–N=N–) bearing aromatic rings, dominates the worldwide market of dyestuffs with a share of about 70% [2]. Reactive dyes are the most common dyes used due to their advantages, such as bright colors, excellent color fastness and ease of application [3,4]. They exhibit a wide range of different chemical structures, primarily based on substituted aromatic and heterocyclic groups. A large number of reactive dyes are azo compounds that are linked by an azo bridge [5]. Many reactive dyes are toxic to some organisms and may cause direct destruction of creatures in water [6]. In addition, since reactive dyes are highly soluble in water, their removal from effluent is difficult by conventional physicochemical and biological treatment methods [7,8].

Batch experiments are usually done to measure the effectiveness of adsorption for removing specific adsorbates as well as to determine the maximum adsorption capacity. The continuous adsorption in fixed-bed column is often desired from industrial point of view. It is simple to operate and can be scaled-up from a laboratory process [9]. A continuous packed bed adsorber does not run under equilibrium conditions and the effect of flow condition (hydrodynamics) at any cross-section in the column affects the flow behaviour downstream. The flow behaviour and mass transfer aspects become peculiar beyond a particular length to diameter ratio of the column [10]. In order to design and operate fixed-bed adsorption process successfully, the breakthrough curves under specified operating conditions must be predictable. The shape of this curve is influenced by the individual transport process in the column and in the adsorbent [11]. Breakthrough determines bed height and the operating life span of the bed and regeneration times [12]. Adsorption in fixed-bed columns using activated carbon has been widely used in industrial processes for the removal of contaminants from aqueous textile industry effluents, since it does not require the addition of chemical compounds in the separation process [13].

Activated carbon adsorption has been found to be superior for wastewater treatment compared to other physical and chemical techniques, such as flocculation, coagulation, precipitation and ozonation as they possess inherent limitations such as high cost, formation of hazardous by-products and intensive energy requirements [14]. However, commercially available activated carbons are still considered expensive [15]. This is due to the use of non-renewable and relatively expensive starting material such as coal, which is unjustified in pollution control applications [16]. Therefore, in recent years, this has prompted a growing research interest in the production of activated carbons from renewable

* Corresponding author. Fax: +60 45941013.
E-mail address: chbassim@eng.usm.my (B.H. Hameed).

and cheaper precursors which are mainly industrial and agricultural by-products. The methods of activation commonly employed can broadly be divided into two main types: thermal (or physical) activation and chemical activation. Thermal activation involves primary carbonization (below 700 °C) followed by controlled gasification under the action of oxidizing gases at high temperature (up to 1100 °C). In chemical activation the precursor is mixed with a chemical restricting the formation of tars (e.g. $ZnCl_2$, H_3PO_4, etc.), after kneading carbonized and washed to produce the final AC. The chemical incorporated into the interior of the precursor particles reacts with the thermal decomposition products reducing the evolution of volatiles and inhibits the shrinkage of the particles. In this way, the conversion of the precursor to carbon is high, and once the chemical is eliminated after the heat treatment, a large internal porosity is formed [17]. Phosphoric acid activation only involves a single heat treatment step and is achieved at lower temperatures (400–600 °C), higher yields are obtained and most of the phosphoric acid can be recovered after the process is completed. The chemical activation of lignocellulosic materials with phosphoric acid has been extensively investigated from the development of porosity [18–21] and mechanism of degradation from the precursor point of view [22,23]. Phosphoric acid incorporated into the interior of the precursor particle restricted the formation of tar as well as other liquids such as acetic acid and methanol and inhibited the particle shrinkage or volume contraction during heat treatment. Phosphoric acid changed or modified the surface chemistry of adsorbent due to the formation of acidic oxygen-contained complexes by strong oxidization [22].

In this work, the removal efficiency of bamboo waste based granular activated carbon (BGAC) used RB5 in the textile industry by fixed-bed column was investigated. The important design parameters such as inlet concentration of dye solution, flow rate of fluid and column bed height [8,24–26] were investigated using a laboratory scale fixed-bed column. The breakthrough curves for the adsorption of RB5 were analyzed using Adam's–Bohart, Thomas and Yoon–Nelson models. Further, modeling on the adsorption dynamics of the fixed bed was presented and finally the correlation between the model and the experimental data was compared.

2. Experimental

2.1. Adsorbate

Chemazol Black B (C.I. Reactive Black 5) (RB5) used in this study was purchased from Sigma–Aldrich (M) Sdn Bhd, Malaysia. RB5 has molecular formula $C_{26}H_{21}N_5Na_4O_{19}S_6$ (Mol. wt. 991.82 g/mol). The maximum wavelength of this dye is 579 nm. The dye stock solution was prepared by dissolving accurately weight dye in distilled water to the concentration of 1 g/L. The experimental solutions were obtained by diluting the dye stock solution in accurate proportions to needed inlet concentrations. The chemical structure of RB5 is shown in Fig. 1.

2.2. Preparation of activated carbon

Bamboo waste used for preparation of granular activated carbon was obtained from local furniture factory, Penang, Malaysia. It was washed with hot distilled water to remove dust like impurities then dried in an oven (Model Memmert 600, Germany) at temperature of 105 °C for 24 h and then crushed and sieved to the desired particle size (1–2 mm). Chemical activation method using phosphoric acid (purity 85% Merck, Germany) was used to activate the raw material. 40 g of precursor was impregnated by certain amount of 40 wt% concentration phosphoric acid with occasional stirring. The amount of phosphoric acid solution used was adjusted to give a certain impregnation ratio (weight of activating agent:weight of

Fig. 1. Molecular structure of the C.I. Reactive Black 5 dye.

precursor) of 4.5:1. This ratio was chosen based on our preliminary work. The impregnation ratio is given by:

$$IR = (\text{weight of phosphoric acid in solution}) : (\text{weight of precursor})$$
(1)

After impregnation, the solution was filtered to take the residual acid. Subsequently, impregnated samples were air dried at under sunlight for 3 days. Activation of phosphoric acid impregnated precursor was carried out at 500 °C and time 2 h under nitrogen flow (150 cm^3/g) at a heating rate of 10 °C/min. After activation, the samples were cooled to room temperature and then washed sequentially several times with hot distilled water (70 °C) until the pH of the washing solution reached 6–7. Finally samples were dried in an oven at 110 °C for 24 h and then stored in plastic containers.

2.3. Experimental set-up

The fixed-bed column was made of Pyrex glass tube of 1.2 cm inner diameter and 19.5 cm height. At the bottom of the column, a stainless steel sieve was attached followed by a layer of glass wool. A known quantity of the prepared activated carbon was packed in the column to yield the desired bed height of the adsorbent 40, 60 and 80 mm (equivalent to 2.09, 3.12 and 4.14 g of activated carbon). The column was then filled up with glass beads in order to provide a uniform flow of the solution through the column. Dye solution of known concentrations (50, 100 and 200 mg/L) at pH 6.5 was pumped upward through the column at a desired flow rate (10, 20 and 30 mL/min) controlled by a peristaltic pump (Masterflex, Cole-Parmer Instrument Co.). The RB5 solutions at the outlet of the column were collected at regular time intervals and the concentration was measured using a double beam UV–visible spectrophotometer (Shimadzu, Japan) at 597 nm. The experiments were carried out at temperature of 28 ± 1 °C without any pH adjustment.

2.4. Analysis of fixed-bed column data

The time for breakthrough appearance and the shape of the breakthrough curve are very important characteristics for determining the operation and the dynamic response of an adsorption fixed-bed column. The breakthrough curves show the loading behavior of dye to be removed from solution in a fixed-bed column and is usually expressed in terms of adsorbed dye concentration (C_{ad}), inlet RB5 concentration (C_o), outlet RB5 concentration (C_t) or normalized concentration defined as the ratio of outlet RB5 concentration to inlet RB5 concentration (C_t/C_o) as a function of time or volume of effluent for a given bed height [22]. Effluent volume (V_{eff}) can be calculated as

$$V_{eff} = Qt_{total}$$
(2)

where t_{total} and Q are the total flow time (min) and volumetric flow rate (mL/min). The area under the breakthrough curve (A)
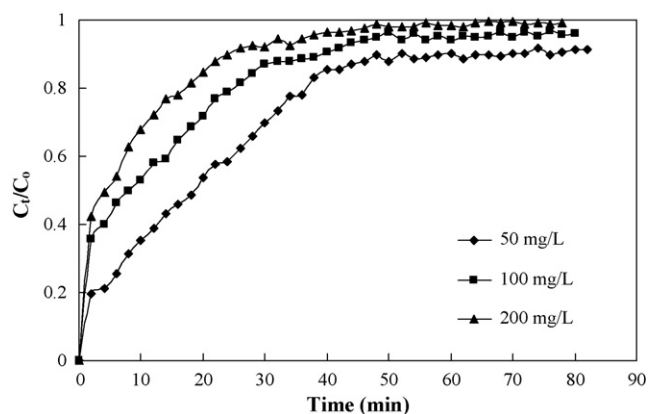
Fig. 2. Breakthrough curves for RB5 adsorption on prepared BGAC at different inlet RB5 concentrations (bed height = 60 mm, flow rate = 10 mL/min, temperature = 28 ± 1 °C).

obtained by integrating the adsorbed concentration (C_{ad}; mg/L) versus t (min) plot can be used to find the total adsorbed RB5 quantity (maximum column capacity). Total adsorbed RB5 quantity q_{total} (mg) in the column for a given feed concentration and flow rate is calculated as [27]:

$$q_{total} = \frac{Q}{1000} \int_{t=0}^{t=t_{total}} C_{ad}\ dt \qquad (3)$$

Equilibrium uptake q_{eq} (mg/g) or maximum capacity of the column in the column is defined by equation (4) as the total amount of adsorbed (q_{total}) per gram of adsorbent (w) at the end of total flow time [27]:

$$q_{eq} = \frac{q_{total}}{w} \qquad (4)$$

3. Results and discussion

3.1. Effect of initial dye concentration

The effect of a variation of the inlet RB5 concentration from 50 to 200 mg/L used with the same adsorbent bed height of 60 mm and solution flow rate of 10 mL/min is shown by the breakthrough curve in Fig. 2. As shown in Fig. 2, in the interval of 50 min, the value of C_t/C_0 reached 0.87, 0.96 and 0.98 when inlet concentration was 50, 100 and 200 mg/L, respectively. It is illustrated that the breakthrough time slightly decreased with increasing inlet RB5 concentration. At lower inlet RB5 concentrations, breakthrough curves were dispersed and breakthrough occurred slower. As influent concentration increased, sharper breakthrough curves were obtained. This can be explained by the fact that a lower concentration gradient caused a slower transport due to a decrease in the diffusion coefficient or mass transfer coefficient. The larger the inlet concentration, the steeper is the slope of breakthrough curve and smaller is the breakthrough time. These results demonstrate that the change of concentration gradient affects the saturation rate and breakthrough time, or in other words, the diffusion process is concentration dependent. As the influent concentration increases, RB5 loading rate increases, so does the driving force increase for mass transfer, which in a decrease in the adsorption zone length [28]. Similar trends were obtained for biosorption of methylene blue by rice husk [25], removal of acid dye using pristine and acid-activated clays [29]. The adsorption capacity was expected to increase with increasing the inlet concentration because a high concentration difference provides a high driving force for the adsorption process. The highest bed capacity of 39.02 mg/g was obtained using 100 mg/L inlet dye concentration, 80 mm bed height and 10 mL/min flow rate.

Table 1
Column data parameters obtained at different inlet RB5 concentrations, bed heights and flow rates ($T = 28 ± 1$ °C).

Inlet concentrations (mg/L)	BGAC bed height (mm)	Flow rate (mL/min)	q_{total} (mg)	q_e (mg/g)
50	60	10	82.05	28.32
100	60	10	81.02	27.67
200	60	10	80.23	26.66
100	80	10	86.53	39.02
100	40	10	78.05	23.43
100	60	20	62.87	20.62
100	60	30	38.91	12.66

The results were in agreement with the works reported previously on various fixed-bed adsorption systems [14,24]. All the adsorption capacities and the exhaustion times obtained are listed in Table 1.

3.2. Effect of the solution flow rate

The effect of the flow rate on the adsorption of RB5 using the BGAC was investigated by varying the flow rate (10, 20 and 30 mL/min) with a constant adsorbent bed height of 6 cm and the inlet RB5 concentration of 100 mg/L, as shown by the breakthrough curve in Fig. 3. It was shown that breakthrough generally occurred faster with higher flow rate. Breakthrough time reaching saturation was increased significantly with a decreased in the flow rate. When at a low rate of inlet RB5 had more time to contact with BGAC that resulted in higher removal of RB5 ions in column. The variation in the slope of the breakthrough curve and adsorption capacity may be explained on the basis of mass transfer fundamentals. The reason is that at higher flow rate the rate of mass transfer gets increases, i.e. the amount of dye adsorbed onto unit bed height (mass transfer zone) gets increased with increasing flow rate leading to faster saturation at higher flow rate [30]. At a higher flow rate, the adsorption capacity was lower due to insufficient residence time of the solute in the column and diffusion of the solute into the pores of the adsorbent, and therefore, the solute left the column before equilibrium occurred. These results were in agreement with those referred to the literatures [31,30].

3.3. Effect of activated carbon bed height

Fig. 4 shows the breakthrough curve obtained for RB5 adsorption on the BGAC for different bed heights of 40, 60 and 80 mm (2.09, 3.12 and 4.14 g), at a constant flow rate of 10 mL/min and RB5 inlet concentration of 100 mg/L. From Fig. 4, both the breakthrough and time increased with increasing the bed height. The bed height
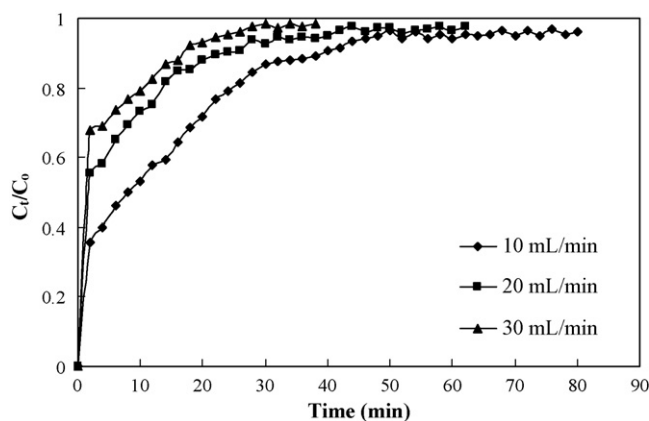

Fig. 3. Breakthrough curves for RB5 adsorption on prepared BGAC at different flow rates (inlet RB5 concentration = 100 mg/L, bed height = 60 mm, temperature = 28 ± 1 °C).
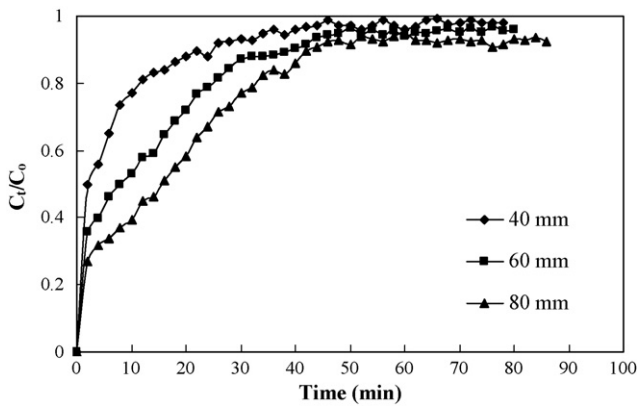
Fig. 4. Breakthrough curves for RB5 adsorption on prepared BGAC at different bed heights (inlet RB5 concentration = 100 mg/L, flow rate = 10 mL/min, temperature = 28 ± 1 °C).

increases, RB5 had more time to contact with BGAC that resulted in higher removal efficiency of RB5 in column. So the higher bed column results in a decrease in the solute concentration in the effluent at the same time. The slope of breakthrough curve decreased with increasing bed height, which resulted in a broadened mass transfer zone. High adsorption capacity was observed at the highest bed height due to an increase in the surface area of adsorbent, which provided more binding sites for the adsorption [32,33]. The total RB5 adsorbed together with the exhaustion times are also listed in Table 1.

3.4. Dynamic adsorption models

3.4.1. The Adam's–Bohart model

Adam's–Bohart model [34] model established the fundamental equations describing the relationship between C_t/C_o and t in a continuous system. The Adam's–Bohart model is used for the description of the initial part of the breakthrough curve. The expression is the following:

$$\ln \frac{C_t}{C_o} = k_{AB}C_o t - k_{AB}N_o \frac{Z}{F} \qquad (5)$$

where C_o and C_t (mg/L) are the inlet and effluent dyes concentration. k_{AB} (L/mg min) is the kinetic constant, F (cm/min) is the linear velocity calculated by dividing the flow rate by the column section

area, Z (cm)is the bed depth of column and N_o (mg/L) is the saturation concentration. A linear plot of $\ln(C_t/C_o)$ against time (t) was determined values of k_{AB} and N_o from the intercept and slope of the plot (figure not shown).

The Adam's–Bohart adsorption model was applied to experimental data for the description of the initial part of the breakthrough curve. After applying Eq. (5) to the experimental data at the 10% breakthrough point, a linear relationship was found when the time for 10% breakthrough ($t_{0.1}$). For all breakthrough curves, respective values of N_o, and k_{AB} were calculated and presented in Table 2 together with the correlation coefficients ($R^2 > 0.73$). From Table 2, it is seen that the values of N_o at all conditions have no significant difference. Although the Adam's–Bohart model provides a simple and comprehensive approach to running and evaluating adsorption-column tests, its validity is limited to the range of conditions used. From Table 2 the values of k_{AB} decreased with both initial RB5 concentration and flow rate increase, but it increased with bed heights increase. This showed that the overall system kinetics was dominated by external mass transfer in the initial part of adsorption in the column [27].

3.4.2. Thomas model

Thomas model [35] assumes plug flow behavior in the bed, and uses Langmuir isotherm for equilibrium, and second-order reversible reaction kinetics. This model is suitable for adsorption processes where the external and internal diffusion limitations are absent. The linearized form of Thomas model can be expressed as follows:

$$\ln \left(\frac{C_o}{C_t} - 1 \right) = \frac{k_{Th}q_o w}{Q} - k_{Th}C_o t \qquad (6)$$

where k_{Th} (mL/min mg) is the Thomas rate constant; q_o (mg/g) is the equilibrium RB5 uptake per g of the adsorbent; C_o (mg/L) is the inlet RB5 concentration; C_t (mg/L) is the outlet concentration at time t; W (g) the mass of adsorbent, Q (mL/min) the flow rate and t_{total} (min) stands for flow time. The value of C_t/C_o is the ratio of outlet and inlet RB5 concentrations. A linear plot of $\ln[(C_o/C_t) - 1]$ against time (t) was employed (figure not shown) to determine values of k_{Th} and q_o from the intercept and slope of the plot.

The column data were fitted to the Thomas model to determine the Thomas rate constant (k_{Th}) and maximum solid-phase concentration (q_o). The determined coefficients and relative constants were obtained using linear regression analysis according to Eq. (6) and the results are listed in Table 3. From Table 3, it is seen that

Table 2
Adam's–Bohart parameters at different conditions using linear regression analysis.

Inlet concentrations (mg/L)	BGAC bed height (mm)	Flow rate (mL/min)	k_{AB} (L/mg min) $\times 10^3$	N_o (mg/L)	R^2
50	60	10	0.766	97.237	0.94
100	60	10	0.245	102.140	0.92
200	60	10	0.098	104.314	0.82
100	80	10	0.302	106.266	0.95
100	40	10	0.132	93.377	0.73
100	60	20	0.139	83.843	0.81
100	60	30	0.104	79.984	0.86

Table 3
Thomas model parameters at different conditions using linear regression analysis.

Inlet concentrations (mg/L)	BGAC bed height (mm)	Flow rate (mL/min)	k_{Th} (mL/min mg) $\times 10^3$	q_o (mg/g)	R^2
50	60	10	1.480	28.520	0.99
100	60	10	0.731	25.260	0.98
200	60	10	0.428	26.323	0.98
100	80	10	0.758	37.840	0.99
100	40	10	0.734	23.530	0.94
100	60	20	0.660	14.460	0.93
100	60	30	1.005	8.390	0.97

Table 4
Yoon–Nelson parameters at different conditions using linear regression analysis.

Inlet concentrations (mg/L)	BGAC bed height (mm)	Flow rate (mL/min)	k_{YN} (1/min)	τ (min)	R^2
50	60	10	0.076	18.878	0.99
100	60	10	0.075	7.956	0.99
200	60	10	0.088	8.881	0.98
100	80	10	0.758	14.931	0.99
100	40	10	0.073	4.707	0.94
100	60	20	0.069	5.309	0.96
100	60	30	0.963	4.219	0.96

values of determined coefficients (R^2) range from 0.932 to 0.993. From Table 3, as the inlet concentration increased the value of q_o decreased but the value of k_{Th} increased. The reason is that the driving force for adsorption is the concentration difference between the dye on the adsorbent and the dye in the solution [27,36]. With flow rate increasing, the value of q_o decreased but the value of k_{Th} increased. As the bed heights increased, the value of q_o increased significantly while the value of k_{Th} decreased significantly. So lower flow rate, lower initial concentration and higher bed heights would increase the adsorption of RB5 on the GBAC column. The Thomas model is suitable for adsorption processes where the external and internal diffusions will not be the limiting step [27].

3.4.3. The Yoon–Nelson model

Yoon and Nelson [37] developed a model based on the assumption that the rate of decrease in the probability of adsorption of adsorbate molecule is proportional to the probability of the adsorbate adsorption and the adsorbate breakthrough on the adsorbent. The Yoon–Nelson a linearized model for a single component system is expressed as:

$$\ln\frac{C_t}{C_o - C_t} = k_{YN}t - \tau k_{YN} \qquad (7)$$

where k_{YN} (1/min) is the rate velocity constant, τ(min) is the time in required for 50% adsorbate breakthrough. A linear plot of $\ln[C_t/(C_o - C_t)]$ against sampling time (t) determined values of k_{YN} and τ from the intercept and slope of the plot (figure not shown). The values of k_{YN} and τ are listed in Table 4. From Table 4, the rate constant k_{YN} increased and the 50% breakthrough time τ decreased with increasing both flow rate and RB5 inlet concentration. With the bed heights increasing, the values of τ increased while the values of k_{YN} decreased. The data in Table 4 also indicated that τ values from the calculation were significantly different compared to experimental results.

Among the Thomas and Yoon–Nelson models, the value of correlation coefficients (R^2) listed in Tables 3 and 4, both of them provide the better fit ($R^2 > 0.93$) to the experimental data at various conditions. In a comparison of values of R^2 and breakthrough curves, both the Thomas and Yoon–Nelson models can be used to describe the behavior of the adsorption of RB5 in a fixed-bed column. The Adam's–Bohart mode is best fitted to the relative concentration up to 0.5 (C_t/C_0). The value of R^2 was slightly lower than Thomas and Yoon–Nelson models under the same experimental conditions. The Adam's–Bohart model is only used for the description of the initial part of the breakthrough curve. Similar observations were reported by the adsorption of Congo red on rice husk [38] and methylene blue by phoenix tree leaf powder in a fixed-bed column [39].

4. Conclusion

This investigation showed that the granular activated carbon prepared from bamboo waste by chemical activation using phosphoric acid was a promising for removing RB5 from aqueous solutions using fixed-bed adsorption column. The fixed-bed adsorption system was found to perform better with lower RB5 inlet concentration, lower feed flow rate and higher activated carbon bed height. The column experimental data were analyzed by the Adam's–Bohart, Thomas and Yoon–Nelson models. For RB5 adsorption, the column data were fitted well to the Thomas and Yoon–Nelson models.

References

[1] J.F. Osma, V. Saravia, J.L. Toca-Herrera, S.R. Couto, Sunflower seed shells: a novel and effective low-cost adsorbent for the removal of the diazo dye Reactive Black 5 from aqueous solutions, J. Hazard. Mater. 147 (2007) 900–905.
[2] G.M.B. Soares, M.T.P. Amorim, R. Hrdina, M. Costa-Ferreira, Studies on the biotransformation of novel diazo dyes by laccas, Process Biochem. 37 (2002) 581–587.
[3] X.Y. Yang, B. Al-Duri, Application of branched pore diffusion model in the adsorption of reactive dyes on activated carbon, Chem. Eng. J. 83 (2001) 15–23.
[4] O.T. Mahony, E. Guibal, J.M. Tobin, Reactive dye biosorption by Rhizopus arrhizus biomass, Enzyme Microb. Technol. 31 (2002) 456–463.
[5] E.K. Raymound, F. Dunald, Encyclopedia of Chemical Technology, Wiley, New York, 1984.
[6] S. Papic, N. Koprivanac, A.L. Bozic, A. Metes, Removal of some reactive dyes from synthetic wastewater by combined Al(III) coagulation/carbon adsorption process, Dyes Pigments 62 (2004), 291–208.
[7] J.M. Chern, S.N. Huang, Study of nonlinear wave propagation theory. 1. Dye adsorption by activated carbon, Ind. Eng. Chem. Res. 37 (1998) 253–257.
[8] M. Ozacar, I.A. Sengil, Adsorption of reactive dyes on calcined alunite from aqueous solutions, J. Hazard. Mater. B 98 (2003) 211–224.
[9] J.M. Chern, Y.W. Chien, Adsorption of nitrophenol onto activated carbon: isotherms and breakthrough curves, Water Res. 36 (2002) 647–655.
[10] S. Singh, V.C. Srivastava, I.D. Mall, Fixed-bed study for adsorptive removal of furfural by activated carbon, Colloids Surf A: Physicochem. Eng. Aspects 332 (2009) 50–56.
[11] G. Vazquez, R. Alonso, S. Freire, J. Gonzalez-Alvarez, G. Antorrena, Uptake of phenol from aqueous solutions by adsorption in a Pinus pinaster bark packed bed, J. Hazard. Mater. B 133 (2006) 61–67.
[12] G.M. Walker, L.R. Weatherley, Adsorption of acid dyes onto granular activated carbon in fixed bed, Water Res. 31 (1997) 2093–2101.
[13] J.M. Chern, Y.W. Chien, Competitive adsorption of benzoic acid and p-nitrophenol onto activated carbon: isotherm and breakthrough curves, Water Res. 37 (2003) 2347–2356.
[14] T.V.N. Padmesh, K. Vijayaraghavan, G. Sekaran, M. Velan, Biosorption of Acid Blue 15 using fresh water macroalga Azolla filiculoides: batch and column studies, Dyes Pigments 71 (2006) 77–82.
[15] C. Sourja, D. Sirshendu, D.G. Sunando, K.B. Jayanta, Adsorption study for the removal of a basic: experimental and modeling, Chemosphere 58 (2005) 1079–1086.
[16] M.J. Martin, A. Artola, M.D. Balaguer, M. Rigola, Activated carbons developed from surplus sewage sludge for the removal of dyes from dilute aqueous solutions, Chem. Eng. J. 94 (2003) 231–239.
[17] B.S. Girgis, A.A. El-Hendawy, Porosity development in activated carbons obtained from date pits under chemical activation with phosphoric acid, Micropor. Mesopor. Mater. 52 (2002) 105–117.
[18] Y. Diao, W.P. Walawender, L.T. Fan, Activated carbons prepared from phosphoric acid activation of grain sorghum, Bioresour. Technol. 81 (2002) 45–52.
[19] M. Jagtoyen, F.J. Derbyshire, Activated carbons from yellow poplar and white oak by H$_3$PO$_4$ activation, Carbon 36 (1998) 1085–1097.
[20] F. Suarez-Garcia, A. Martinez-Alonso, J.M.D. Tascon, Pyrolysis of apple pulp: chemical activation with phosphoric acid, J. Anal. Appl. Pyrol. 63 (2002) 283–301.
[21] T. Vernersson, P.R. Bonelli, E.G. Cerrella, A.L. Cukierman, Arundo donax cane as a precursor for activated carbons preparation by phosphoric acid activation, Bioresour. Technol. 83 (2002) 95–104.

[22] J. Guo, A.C. Lua, Textural and chemical properties of adsorbent prepared from palm shell by phosphoric acid activation, Mater. Chem. Phys. 80 (2003) 114–119.

[23] M.S. Solum, R.J. Pugmire, M. Jagtoyen, F. Derbyshire, Evolution of carbon structure in chemically activated wood, Carbon 33 (1995) 1247–1254.

[24] I.A.W. Tan, A.L. Ahmad, B.H. Hameed, Adsorption of basic dye using activated carbon prepared from oil palm shell: batch and fixed bed studies, Desalination 225 (2008) 13–28.

[25] R. Han, Y. Wang, W. Yu, W. Zou, J. Shi, H. Liu, Biosorption of methylene blue from aqueous solution by rice husk in a fixed-bed column, J. Hazard. Mater. 141 (2007) 713–718.

[26] R. Han, Y. Wang, X. Zhao, Y. Wang, F. Xie, J. Cheng, M. Tang, Adsorption of methylene blue by phoenix tree leaf powder in a fixed-bed column: experiments and prediction of breakthrough curves, Desalination 245 (2009) 284–297.

[27] Z. Aksu, F. Gonen, Biosorption of phenol by immobilized activated sludge in a continuous packed bed: prediction of breakthrough curves, Process Biochem. 39 (2004) 599–613.

[28] J. Goel, K. Kadirvelu, C. Rajagopal, V.K. Garg, Removal of lead(II) by adsorption using treated granular activated carbon: batch and column studies, J. Hazard. Mater. B 125 (2005) 211–220.

[29] S.H. Lina, R.S. Juangb, Y.H. Wang, Adsorption of acid dye from water onto pristine and acid-activated clays in fixed beds, J. Hazard. Mater. B 113 (2004) 195–200.

[30] D.C.K. Ko, J.F. Porter, G. McKay, Optimised correlations for the fixed-bed adsorption of metal ions on bone char, Chem. Eng. Sci. 55 (2000) 5819–5829.

[31] V.C. Taty-Costodes, H. Fauduet, C. Porte, Y.S. Ho, Removal of lead(II) ions from synthetic and real effluents using immobilized Pinus svlvestris sawdust: adsorption on a fixed column, J. Hazard. Mater. B 123 (2005) 135–144.

[32] Z. Zulfadhly, M.D. Mashitah, S. Bhatia, Heavy metals removal in fixed-bed column by the macro fungus *Pycnoporus sanguineus*, Environ. Pollut. 112 (2001) 463–470.

[33] K. Vijayaraghavan, J. Jegan, K. Palanivelu, M. Velan, Removal of nickel(II) ions from aqueous solution using crab shell particles in a packed bed up flow column, J. Hazard. Mater. 113 (1–3) (2004) 223–230.

[34] G.S. Bohart, E.Q. Adams, Behavior of charcoal towards chlorine, J. Chem. Soc. 42 (1920) 523–529.

[35] H.C. Thomas, Heterogeneous ion exchange in a flowing system, J. Am. Chem. Soc. 66 (1944) 1466–1664.

[36] T.V.N. Padmesh, K. Vijayaraghavan, G. Sekaran, M. Velan, Batch and column studies on biosorption of acid dyes on fresh water macro alga *Azolla filiculoides*, J. Hazard. Mater. B 125 (2005) 121–129.

[37] Y.H. Yoon, J.H. Nelson, Application of gas adsorption kinetics. Part 1. A theoretical model for respirator cartridge service time, Am. Ind. Hyg. Assoc. J. 45 (1984) 509–516.

[38] R. Han, D. Ding, Y. Xu, W. Zou, Y. Wang, Y. Li, L. Zou, Use of rice husk for the adsorption of congo red from aqueous solution in column mode, Bioresour. Technol. 99 (2008) 2938–2946.

[39] R. Hana, Y. Wanga, X. Zhaoc, Y. Wanga, F. Xieb, J. Chengb, M. Tang, Adsorption of methylene blue by phoenix tree leaf powder in a fixed-bed column: experiments and prediction of breakthrough curves, Desalination 245 (2009) 284–297.